

THE IMPACT OF ACTIVE NOISE CONTROL ON THE PERCEIVED SOUND QUALITY

Leopoldo P. R. de Oliveira; Paulo Sergio Varoto

Universidade de São Paulo – Escola de Engenharia de São Carlos, Lab. de Dinâmica
Av. Trabalhador Sancarlense, 400 – 13566-590 São Carlos-SP, Brasil
leopro@sc.usp.br; varoto@sc.usp.br

Paul Sas; Wim Desmet

Katholieke Universiteit Leuven - Department of Mechanical Engineering
Celestijnenlaan 300B B-3001 Leuven - Belgium
paul.sas@mech.kuleuven.be; wim.desmet@mech.kuleuven.be

Peter Mas; Herman Van der Auweraer

LMS International
Interleuvenlaan 68, B – 3001 Leuven, Belgium
peter.mas@lmsintl.com; herman.vanderauweraer@lmsintl.com

Abstract. *Active noise control solutions appears to be a feasible approach to cope with the steadily increasing requirements for noise reduction and, more recently, for sound quality improvement in the transportation industry. Active controllers tend to be designed with a target on the noise pressure level reduction. However, the perceived sound field for the occupant can be more accurately accessed if psychoacoustic metrics, such as specific loudness are taken into account. Therefore, through a simulation methodologies that allows the use of structural and acoustical sensors and actuators in a fully coupled vibro-acoustic model, the performance of an active noise control system is evaluated in terms of sound quality metrics. For better accuracy, the dynamics of sensors and actuators can also be included, as they can significantly affect the control stability and performance. The modeling procedure is experimentally validated. The system under study consists of a simplified car geometry in real scale, with a flexible firewall that allows a disturbance noise in the engine compartment to be transmitted to the passenger compartment. An engine-like noise disturbance is created with a calibrated low frequency sound source, which is placed in the engine compartment. The acoustic performance is accessed through microphones placed near the occupants' head positions. The controller consists of decentralized units of collocated sensor/actuator pairs placed on the flexible firewall. It is shown that the use of a quite simple control strategy, such as a velocity feedback, besides the advantages on implementation and guaranteed stability, can bring satisfactory results for noise reduction and also for the occupant perceived sound field, as specific loudness and tonality are significantly reduced.*

Keywords: *vibro-acoustic modeling, active noise control, sound quality*

1. INTRODUCTION

The successful development of new products relies on the capability of quantitatively assessing the performance of conceptual design alternatives in an early design phase. In recent years, major progress was made hereto, based on the extensive use of a virtual prototyping. The cornerstone in this framework is to account for the human perception when defining product performance criteria.

Additionally, active control has shown the potential to enhance systems dynamic performance which allows lighter and improved products. Research done in the last years on smart materials and control concepts has led to exploring practical applications with promising results for automotive applications (Van der Auweraer *et al.* 2006).

However, to make the step to 'active sound quality design', the abovementioned schemes need design procedures to become part of the product development process. In other words, this requires: (i) the product performance to be based on human perception attributes and (ii) the simulation models to support the specific aspects related to smart materials (active systems, actuators, sensors and control logic).

In order to demonstrate the proposed modeling procedure, the Sound Brick set-up at LMS.International was selected. It consists of a simplified car cavity, built in concrete to ensure acoustic boundary condition, thus avoiding uncertainties during the vibro-acoustic modeling phase. A previous version of the setup is shown in Fig.1a. The current configuration has a flexible firewall and a rigid engine compartment (EC) as in Fig.1b. A sound source placed in the EC works as a primary disturbance source. The firewall is assembled between the EC and the passenger compartment (PC) which allows a set of structural sensors and actuators to realize the control signals for increasing the transmission loss through these cavities. The PC main dimensions are about 3400 x 1560 x 1270mm; for the EC, 900 x 1100 x 750mm and the firewall 920 x 545 x 1.5mm. Collocated accelerometers and inertia-shakers are used as structural sensors/actuators pairs (SAPs).

The active control scheme adopted is a decentralized velocity feedback controller with structural sensors and actuator. This choice is made upon the advantages of such a scheme with respect to implementation, stability and reliability to system modification (or uncertainties). It is important however to mention that different kinds of control strategies can be adopted under the same simulation framework, which in the end, reveals the functionality of such an approach to the assessment of conceptual design performance.

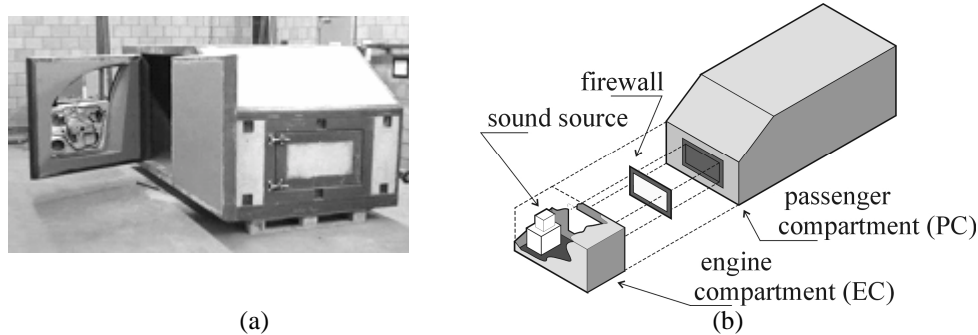


Figure 1 – System under investigation (a) photo (b) schematic view

2. SOUND QUALITY METRIC

Sound quality is the science that studies the human appreciation to a determined auditory stimulus. More than the mathematical interpretation of pressure signals, sound quality and psychoacoustics try to correlate acoustic stimuli with hearing sensation (Zwicker and Fastl, 1999; Fastl, 2005).

In engineering, when approaching a new problem, one tends to use standard tools in order to model, simplify and describe it in a systemic way. As far as sound is concerned, one of the most known functions is the sound pressure level (SPL) either in decibels (dB) or in its filtered forms dBA, dBB, dBC, etc.; or even, if more detailed information about the frequency content is needed, a frequency spectra or a time-frequency plots are used. For example, Fig. 2(a) and (b) depict, respectively, the time history and the frequency spectrum of a pressure signal. The analysis of these two plots, reveals a repetitive and quite tonal behavior of this signal; however, not much about human appreciation can be concluded. A time-frequency plot (Fig. 2c) reveals how frequency components are spread over time with a certain pattern, but arguably, just a very experienced person could predict its nature. Finally, Fig. 2(d) reveals the real nature of that pressure signal, but again, only a person trained in reading this ‘medieval time-frequency diagram’ can anticipate how it would feel like to actually hear it.

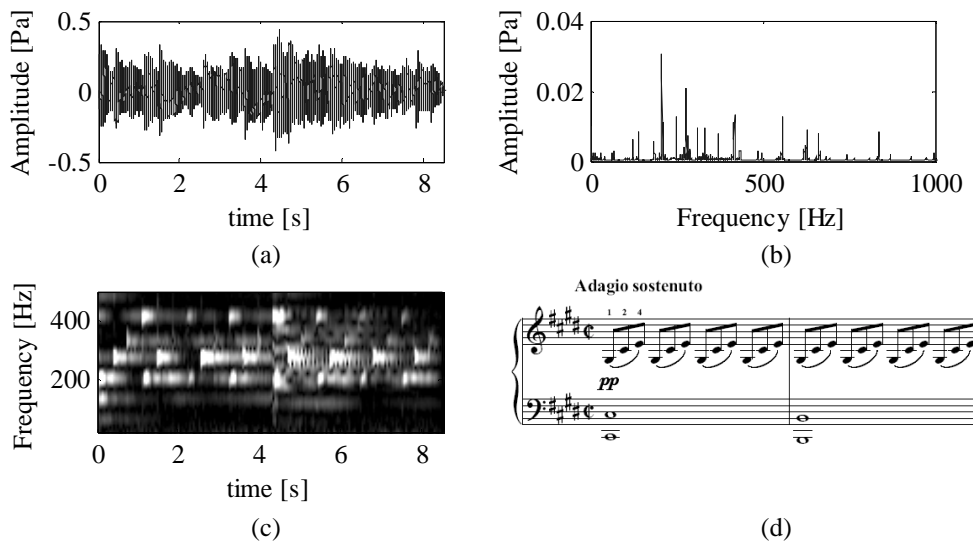


Figure 2 – Various representations of the first bars in the *Sonata Op.27 No.2* from Ludwig van Beethoven: (a) time history, (b) frequency spectrum, (c) time-frequency plot and (d) piano partition

None of the aforementioned tools are easily correlated to the human perception. In fact, the A-, B-, C- and D-weighting filters are an early attempt to include the human ear dynamics into sound measurement and analysis. Those filters were designed to resemble the human hearing sensitivity in the frequency domain (equal loudness contours).

Since this sensitivity is amplitude dependent, each filter is optimized for a certain amplitude range (Sas, 2002), e.g., the A-weighting filter corresponds nearly to the 30Phon curve (30dB @ 1000Hz). In spite showing some correlation with actual human perception, and so being widely used, dBA measurements simply superimpose the effects of different frequency components. In this sense, it neglects an important mechanism within the ear transduction of pressure fluctuations into electrical signal to the brain, namely frequency masking (Zwicker and Fastl, 1999).

Masking has to do with the way hair-cells are positioned in the cochlea, so that a tonal (or narrow band) stimulus excites a specific region in the cochlea with effects on its neighborhood, turning them insensitive to lower levels of excitation, which rises the concept of critical bands of excitation measured in Bark (Zwicker and Fastl, 1999). This phenomenon is responsible, for instance, to the way speech intelligibility is affected by background noise; the capability of recognizing a specific sound (test sound) in the presence of another one (masker sound) is very much related to their relations in level and spectral content. Indeed, masking can be interpreted as the variation on the hearing threshold curve to a test sound in the presence of a masker, i.e., if the test sound spectrum lies below the masked threshold it will be completely inaudible. In that case, while being inaudible, it would still be computed by a SPL-meter, which raised the need for alternative ways of estimating the human perception to the sound level such as the ISO standardized *Specific Loudness* (ISO 532a and ISO 532b).

From the available techniques, only the method developed by Zwicker and Fastl (1999) is valid to broad band excitation, with or without tonal components in free and diffuse fields (Van der Auweraer and Wyckaert, 2005). As depicted in Fig. 2, the first step in the numerical procedure consists of filtering the signal with 1/3-octave filters, which is the first advantage of the method since those filters are standardized and present in many data acquisition and sound level meter systems. In a second step the data is converted from 1/3-octaves to critical bands followed by the masking check. In this stage, if the proceeding band level follows under the making curve of the preceding one, this value is neglected; otherwise the value is kept. Following this procedure, the Specific Loudness graph is obtained with units *Sones/Bark*. The value for Zwicker Loudness is defined as the integral of the Specific Loudness over Bark, with values expressed in *Sones*. The advantage of the *Sones* scale is its linear correlation with the human level perception, i.e., an acoustic stimulus of 4Bark sound twice as low as an 8Bark stimulus.

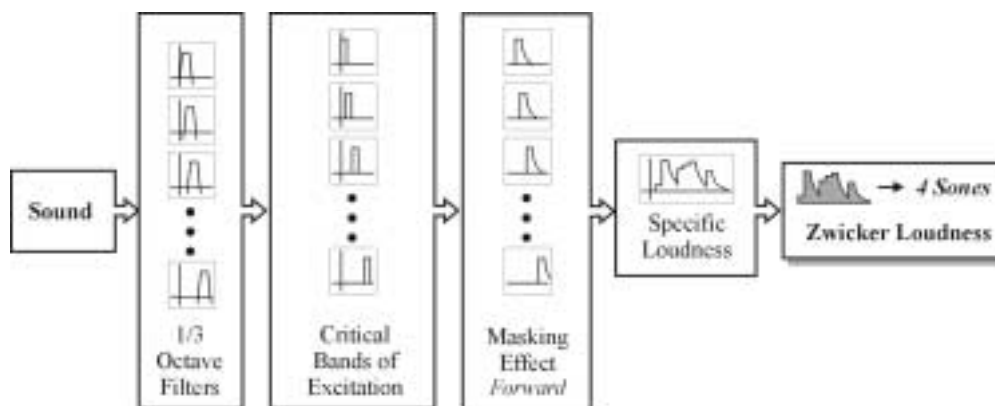


Figure 3 – Numerical procedure scheme for Zwicker Loudness calculation

3. MODELLING PROCEDURE AND CONTROL STRATEGY

Usually, the low frequency noise is transmitted into the vehicle’s cabin through structural paths, which raises the necessity of dealing with vibro-acoustic models. This kind of models allows the use of acoustic disturbance and even secondary sources. The challenge resides in deriving reasonable sized models that incorporate structural and acoustic components integrated with controller algorithm. Oliveira *et al.* (2007) preset a methodology to obtain such reduced models including sensors and actuators dynamics. The final models are presented in a state-space form which allows time-domain computation, hence providing an ideal environment for SQ analysis.

The next sections describe the modeling procedure and present an experimental validation for the reduced state-space models.

3.1 Modelling procedure

The procedure is based on a modal model of the coupled system. It starts with the structural FE model, to which the structural influence of placing sensors and actuators (mass and/or stiffness loads) is taken into account before a modal base is extracted. This modal base is then used, together with the acoustic FE modal base, to calculate the coupled vibro acoustic modal base. In a further step, the vibroacoustic state-space model is derived from the coupled modal base.

The structural mesh is shown in Fig. 4(a) with a total of 231 nodes and 200 elements (4-noded shell elements). The steel firewall, 1.5mm thick, presents 13 modes from 0 to 200Hz and the higher order mode is the [5,2] well described by this number of elements. The inclusion of sensors and actuators mass (and/or stiffness) loading takes place in this step, by adding some concentrated mass to the nodes where those devices are sited.

If the SAP electro-mechanical dynamics are considered to be negligible, this modal based state-space model already allows the implementation of control systems with idealized inputs and outputs. Some preliminary results can be achieved with such models, although a more accurate access to the controller performance requires the inclusion of the secondary path dynamics, which, in this case, will take place in the controller design environment (Matlab/Simulink).

The acoustic mesh with some 30000 nodes and 25000 hexahedral elements is depicted in Fig. 4(b). With respect to the elements size, this acoustic model is valid until 308Hz, considering 10 elements per wavelength (514Hz with 6 elem./wavelength), which is fairly suitable for this application.

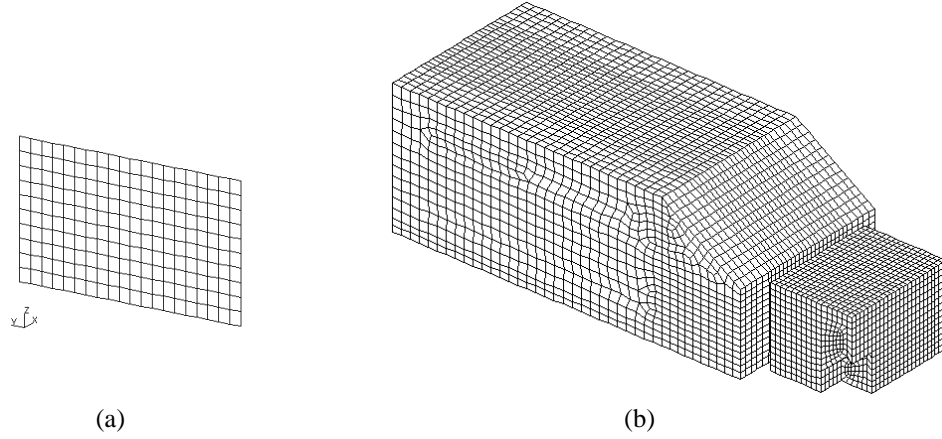


Figure 4 – FE meshes: (a) firewall and (b) acoustic cavities

A fully coupled FE/FE model is adopted. Using the Eulerian formulation, the differential equations for such system can be written as:

$$\left(\begin{bmatrix} \mathbf{K}_s & \mathbf{K}_c \\ \mathbf{0} & \mathbf{K}_a \end{bmatrix} + j\omega \begin{bmatrix} \mathbf{C}_s & \mathbf{0} \\ \mathbf{0} & \mathbf{C}_a \end{bmatrix} - \omega^2 \begin{bmatrix} \mathbf{M}_s & \mathbf{0} \\ -\rho_a \mathbf{K}_c^T & \mathbf{M}_a \end{bmatrix} \right) \begin{Bmatrix} \mathbf{u} \\ \mathbf{p} \end{Bmatrix} = \begin{Bmatrix} \mathbf{F}_s \\ \mathbf{F}_a \end{Bmatrix} \quad (1)$$

where \mathbf{K} , \mathbf{C} and \mathbf{M} are respectively the structural stiffness, damping and mass matrices, the indexes s and a denotes , respectively, structural and acoustic components, \mathbf{K}_c is the coupling matrix, \mathbf{u} is the vector of structural displacements, \mathbf{p} is the vector of acoustic pressures and \mathbf{F} represents the load vectors.

Eventually, the structural and acoustic models are fully-coupled in this FE/FE approach. The effect of the interfacing fluid on the structure dynamics can be considered as a pressure load on the wet surface, whereas the structural vibration works as an extra acoustic input.

Based on Eq. (1) it is clear that the resulting vibro-acoustic system is indeed coupled, though it is not symmetric. The main outcome of such non-symmetric nature is that the eigenproblem associated to this modified FE model is also non-symmetric, hence resulting in distinct left and right eigenvectors.

Since the damping matrix is uncoupled, a normal mode computation can handle this problem. Moreover, it has been indicated by Luo & Gea (1997) that, particularly for the Eulerian formulation (Eq.1), the left and right eigenvector, denoted here respectively by Φ_L and Φ_R can be related as:

$$\Phi_L = \begin{Bmatrix} \Phi_{Ls} \\ \Phi_{La} \end{Bmatrix} = \begin{Bmatrix} \Phi_{Rs} \Omega^2 \\ \Phi_{Ra} \end{Bmatrix} \quad (2)$$

When a coupled modal analysis is performed in LMS.Sysnoise, the resultant modal base is actually the right eigenvectors. Thanks to the relation in Eq.(2) it is possible to retrieve the left eigenvectors to build the complete modal model, which will be the base for the state space formulation described in more detail in a further section.

Therefore, starting from the system generalized state space representation, Eq. (1) yields:

$$\dot{\mathbf{x}} = \begin{bmatrix} \mathbf{0} & \mathbf{I} \\ -\mathbf{M}^{-1}\mathbf{K} & -\mathbf{M}^{-1}\mathbf{C} \end{bmatrix} \mathbf{x} + [b]\mathbf{F}, \quad \mathbf{y} = [c]\mathbf{x} \quad (3)$$

where \mathbf{M} , \mathbf{C} and \mathbf{K} are, respectively, the global mass, damping and stiffness matrices, \mathbf{x} is the vector of states, \mathbf{F} is the load vector, \mathbf{y} is the output vector and $[b]$ and $[c]$ are rectangular matrices with ones on the desired DoFs positions and zeros everywhere else. It is possible to project Eq.(3) to the left and right eigenvectors from eigenvalue problem in Eq.(4) to find the reduced system in Eq.(5):

$$\Phi_L^T \mathbf{M} \Phi_R = \mathbf{I} \quad \text{and} \quad \Phi_L^T \mathbf{K} \Phi_R = \Omega^2 \quad (4)$$

$$\begin{cases} \dot{\mathbf{q}} \\ \ddot{\mathbf{q}} \end{cases} = \begin{bmatrix} \mathbf{0} & \mathbf{I} \\ -\Omega^2 & -\Gamma \end{bmatrix} \begin{cases} \mathbf{q} \\ \dot{\mathbf{q}} \end{cases} + \begin{bmatrix} \mathbf{0} \\ \Phi_L^T [b] \end{bmatrix} \mathbf{F} \quad (5)$$

$$\mathbf{y} = \begin{bmatrix} [c]\Phi_R & \mathbf{0} \end{bmatrix} \begin{cases} \mathbf{q} \\ \dot{\mathbf{q}} \end{cases}$$

Equation (7) shows the modal formulation after the modal expansion in terms of the coupled right eigenvectors furnished by LMS.Sysnoise (Eq.6):

$$\begin{Bmatrix} \mathbf{u} \\ \mathbf{p} \end{Bmatrix} = \sum_{r=1}^{Nc} q_r \begin{Bmatrix} r \Phi_{R s} \\ r \Phi_{R a} \end{Bmatrix} = \Phi_R \mathbf{q} \quad (6)$$

$$\left(\tilde{\mathbf{K}} + j\omega \tilde{\mathbf{C}} - \omega^2 \tilde{\mathbf{M}} \right) \mathbf{q} = \tilde{\mathbf{F}} \quad (7)$$

where $\tilde{\mathbf{K}}$, $\tilde{\mathbf{C}}$ and $\tilde{\mathbf{M}}$ are the modal stiffness, damping and mass matrices, \mathbf{q} is the vector of modal amplitudes and $\tilde{\mathbf{F}}$ is defined as:

$$\tilde{\mathbf{F}} = \Phi_L^T \begin{Bmatrix} \mathbf{F}_s \\ \frac{1}{\rho} \mathbf{F}_a \end{Bmatrix} \quad (8)$$

Since the left eigenvector can be calculated based on the right eigenvector (Eq.2), the modal formulation can be applied to the state space formulation in Eq. (5). In this way the second order system in Eq.(1) can be represented in the following first order state-space form:

$$\dot{\mathbf{x}} = \begin{bmatrix} \mathbf{0} & \mathbf{I} \\ -\tilde{\mathbf{M}}^{-1}\tilde{\mathbf{K}} & -\tilde{\mathbf{M}}^{-1}\tilde{\mathbf{C}} \end{bmatrix} \mathbf{x} + [b]\tilde{\mathbf{F}}, \quad \mathbf{y} = [c]\mathbf{x} \quad (9)$$

where the state vector \mathbf{x} is defined by the modal amplitudes:

$$\mathbf{x} = \begin{bmatrix} \dot{\mathbf{q}} \\ \mathbf{q} \end{bmatrix} \quad (10)$$

3.2 Experimental Validation

In order to validate the model reduction technique, a set of frequency response functions (FRFs), comprising structural and acoustic inputs and outputs, have been measured. As depicted in Fig. 5(a), the structural excitation is performed with a LDS shaker (model V201/3), the force transducer is a PCB 208C04 and the accelerometers are PCB 352C67. Figure 5(b) shows the LMS acoustic source (model E-LMFVVS) placed at the engine compartment. The microphones used are B&K 4188. The vibroacoustic system has been excited with white noise. For the FRF estimation, input and output signals were filtered with hanning windows.

Figure 6 shows a comparison between the experimental and the state-space (SS) FRFs. The material properties adopted after model updating were: speed of sound $c_o = 344,7\text{m/s}$, air density $\rho_o = 1.185\text{kg/m}^3$, firewall density (steel) $\rho = 7800\text{kg/m}^3$ and elasticity modulus $E = 2,33 \cdot 10^{11}\text{Pa}$. As it can be seen, the resultant FRFs present a good agreement.

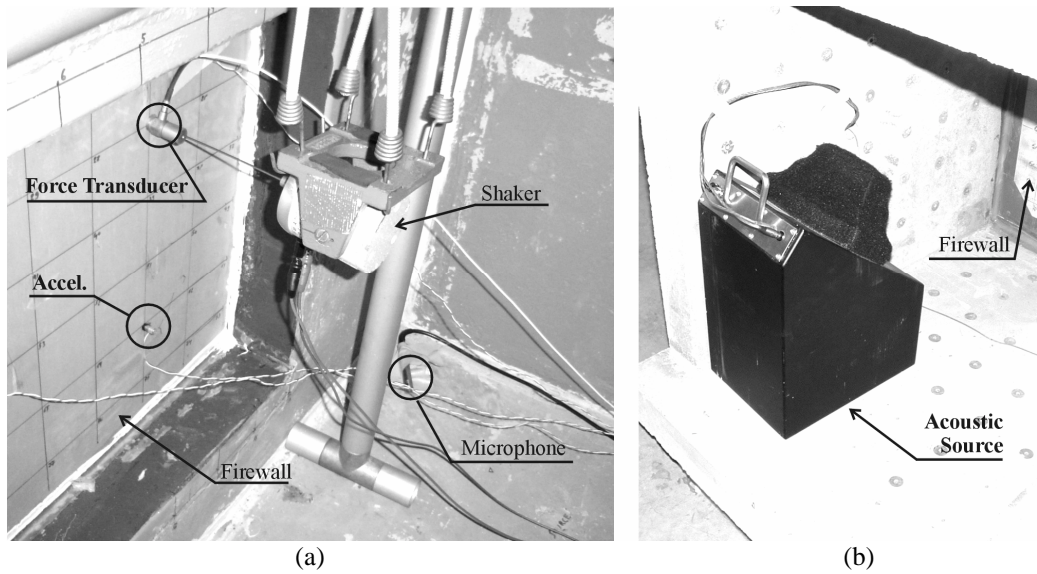


Figure 5 – Experimental setup: (a) view from the passenger compartment with shaker and sensors and (b) view from the engine compartment with sound source

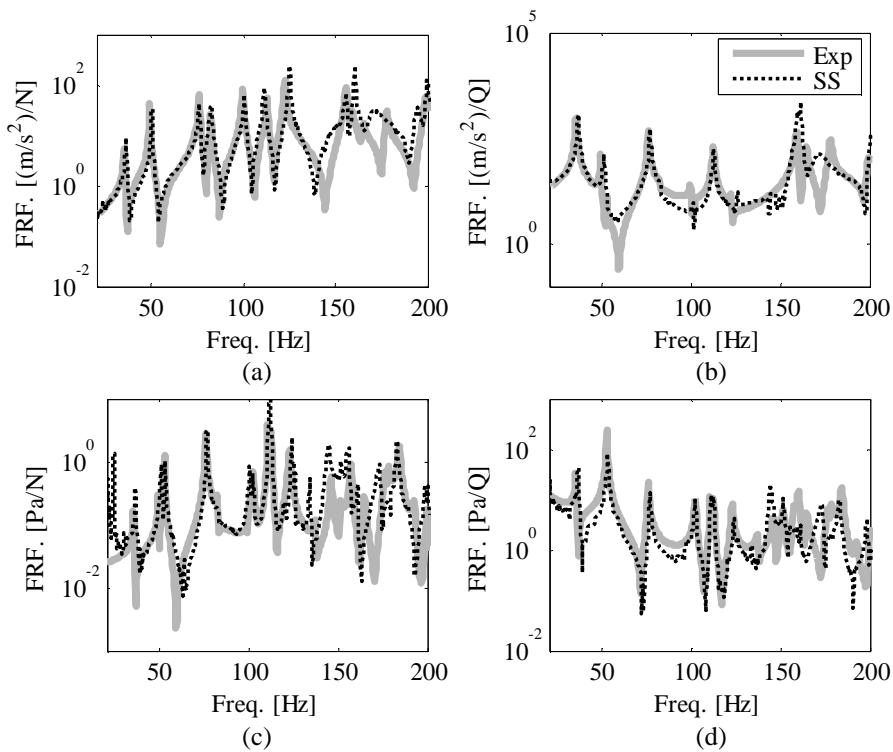


Figure 6 – Comparison between experimental and reduced model FRFs for several output/input relations: (a) struc./struc., (b) struc./acoust., (c) acoust./struc. and (d) acoust./acoust.

3.3 Control Strategy

The proposed control strategy consists of collocated sensor/actuator pairs (SAP) in a decentralized velocity-feedback control loop applied to the firewall. One of the main advantages of such decentralized configuration, when compared to a system with a central control unit, is the relatively simple and economic implementation, still with

satisfactory performance (Baumann *et al.*, 2004). The basic principle of the controller is to feedback the actuator (inertia-shaker) with an amplified voltage proportional to the velocity measured by the collocated sensor. Since the quantity fed back is velocity and the SAP is collocated, i.e., the SAP transfer function presents alternating poles and zeros (Fig. 6a), it can be proven that the control system acts like a passive system and stability is always guaranteed (Preumont, 2002), independent of the feedback gain. However, the value of the feedback gain plays an important role in the achievable performance, which can be targeted to vibration (Engels *et al.*, 2004), radiated sound power (Henriouille and Sas, 2003), or to the sound transmission loss (Oliveira *et al.*, 2006) as in this case.

The interior acoustics of a car can be significantly changed by common actions, such as opening a window or placing more people inside the vehicle. The choice of using only structural elements in the control loop has to do with those uncertainties: due to the relatively weak vibro-acoustic coupling presented by these systems (as it is the case of structure under study), the structural transfer functions (Fig. 6a) are much less sensitive to typical changes in the acoustic components. Despite using only structural sensing and actuation, the control loop gains can be tuned with respect to the acoustic performance.

As mentioned before, in order to have a more accurate prediction of the closed-loop performance of the active solution, the dynamics of actuators and/or sensors should be included in the control system model. Oliveira *et al.* (2007) present a methodology to include inertia shaker models in the control design environment Matlab/Simulink (Fig. 9). The advantage of having the secondary path modeled in such a way resides in the time saved in re-computing the whole system modeling, every time the SAP position (or even type) is changed. As a result, accurate time-domain performance can be evaluated, based on the model reduction technique presented, which is suitable for sound quality assessment.

Figure 7 shows the block diagram of such active noise control model. The state-space model comprises the fully coupled vibroacoustic system. Its multiple inputs and outputs can be connected according to the control strategy adopted. In this case structural sensing and actuation are collocated and decentralized. The shaker model has the SAP driving point displacement and input voltage as inputs, and actuation force as output. For the control realization, the input voltage is taken as the amplified velocity at the SAP location. The amplification factor (feedback gain) can be set to result in maximum attenuation at the target point, in this case, the pressure at the driver's ear location.

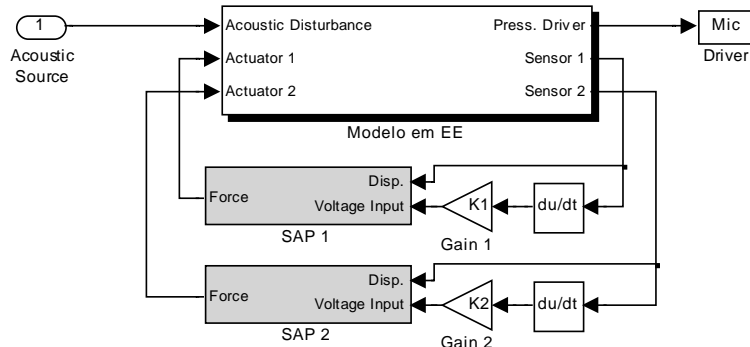


Figure 7 - Block diagram for active noise control simulation with 2 collocated SAPs

4. RESULTS

Based on the modeling procedure described before, simulations were carried out in order to access the effect of the control action on the perceived sound. Two different sound samples were used as acoustic disturbance: a synthesized and a recorded engine noise. The time-frequency plots for the noise stimuli, i.e., the sound samples fed to the volume velocity source in the EC are shown in Fig. 8. The synthesized engine noise (Fig. 8a) is generated by a sound quality equivalent (SQE) engine model, provided by LMS.Virtual Car Sound (Janssens, 2004). The signal in Fig. 8(b) was recorded from a Ford Mondeo with 4 cylinder 2.0l diesel engine in a cycle of accelerations without external load.

The results obtained with both excitation types should provide a consistent set of data from which general conclusions can be taken. Initially, the run-up provides a wide-spectrum excitation evenly distributed in frequency and time. The use of a simulation toll to generate this signal allows a reputable and quite controllable signal profiling without losing the subjectivity of its nature due to the SQ equivalence to a real engine. Additionally, the use of a recorded engine noise allows the assessment of the control performance in a real case scenario, by means of a hybrid (simulation/experimental) computation.

The resultant sound pressure at the driver's head position due to both excitation types are depicted in Fig. 9. As it can be seen, in both cases, the response signals present some characteristic horizontal lines, related to the system resonance frequencies. Also, the low damping of the open loop system can be observed, as particular frequencies remain with considerable amplitude after being excited, giving the plot a horizontal blur characteristic.

When active control is considered, the resultant pressure at the driver's head position is changed to the one depicted in Fig. 10. A qualitative comparison between Figs. 9 and 10 reveals the overall reduction in the noise pressure level (as color scale is kept the same). The aforementioned horizontal blur is also minimized, indicating that the controller introduced damping to the system.

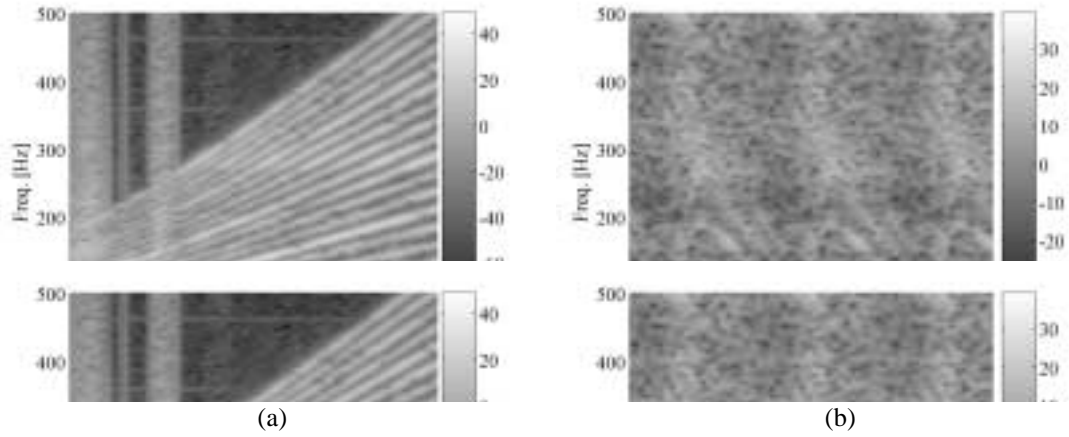


Figure 8 – Time-frequency plots for noise stimuli: (a) synthesized engine run-up and (b) recorded engine noise

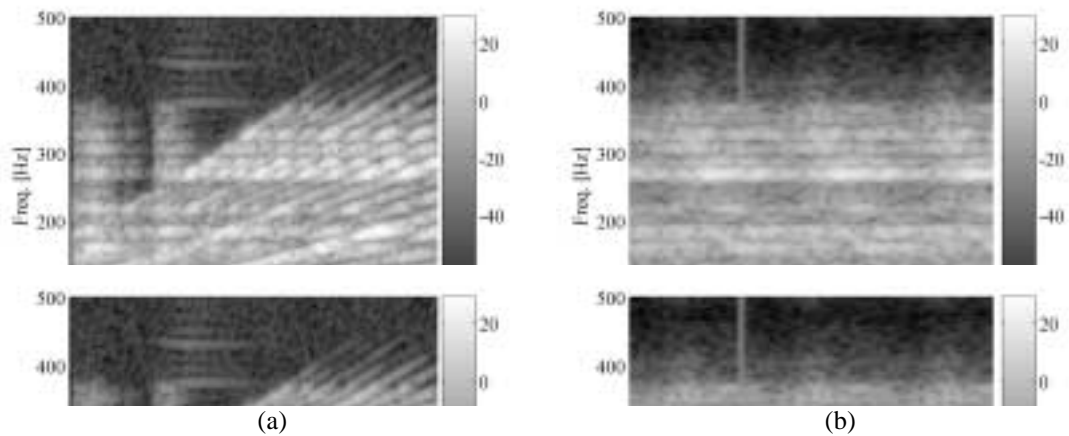


Figure 9 – Time-frequency plots for noise at driver's head position without control: (a) synthesized engine run-up and (b) recorded engine noise

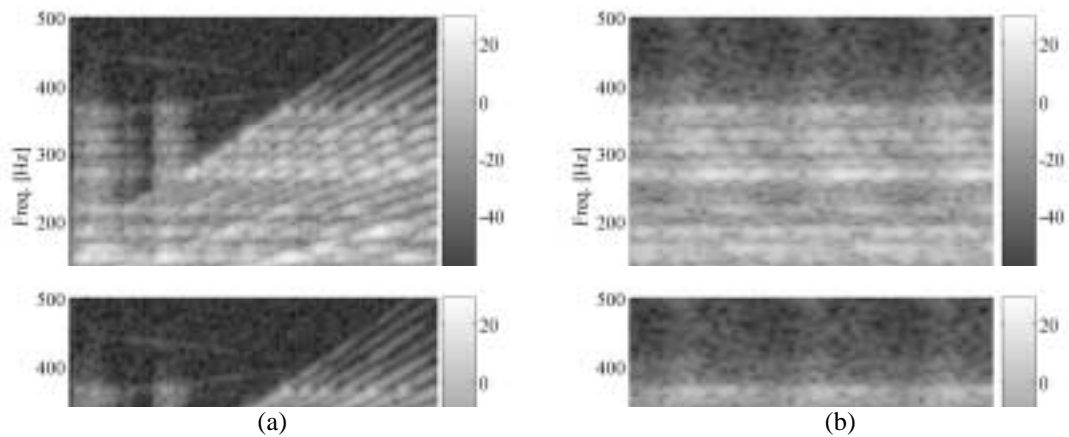


Figure 10 – Time-frequency plots for noise at driver's head position with control: (a) synthesized engine run-up and (b) recorded engine noise

The SPL can be calculated in each case and the results are presented in Tab. 1. As it can be seen, the overall reduction obtained with the synthesized run-up and the recorded engine noise are compatible. However, this information alone does not give a precise prediction of the actual human perception of the control action. In order to obtain a value linearly correlated to the human sensation of volume, the specific loudness was calculated for each of the pressure fields perceived by the driver.

Table 1 – Sound pressure level and Zwicker loudness at the driver’s head position before and after control

SPL [dB]	open-loop	closed-loop	reduction
synthesized engine noise	83.0	76.2	6.8
recorded engine noise	84.5	78.2	6.3

Based on the specific loudness graphs, the Zwicker loudness values were obtained. The latter is given by the integral of the former over the critical bandwidths. Figure 11 compares the specific loudness curves for the open and closed loop responses. As it can be seen, the control system shows more efficiency in low frequency range, up to 2Bark, and still presents reduction up to 3.5Bark. Also, due to the truncation of the reduced modal model, the responses decay after 4Bark.

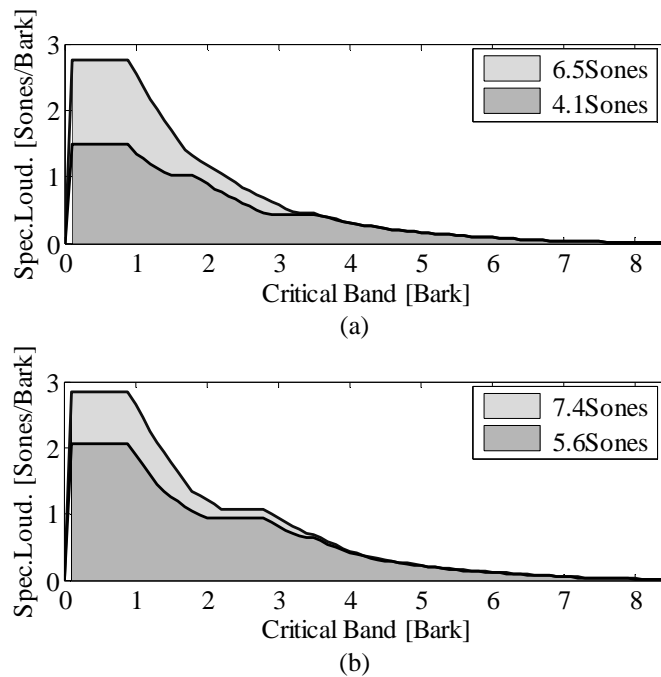


Figure 11 – Comparison between specific loudness contours and Zwicker loudness values for open loop (light gray) and closed loop (dark gray) systems: (a) synthesized engine run-up and (b) recorded engine noise

For the synthesized engine noise, the reduction presented in terms of Zwicker loudness is 2.4Sones, and since this quantity is linearly related to the sensation of volume, it can be said that the sound after control is perceived 63% as loud as the original stimulus. The same analysis performed with the recorded engine noise reveals a 1.8Sones reduction after control, or in this case, the equivalent of 76% of the original loudness. These values are depicted in Tab. 2 for each excitation type, with and without control.

Table 2 – Sound pressure level and Zwicker loudness at the driver’s head position before and after control

Zwicker Loudness [Sones]	open-loop	closed-loop	Reduction
synthesized engine noise	6.5	4.1	2.4 (37%)
recorded engine noise	7.4	5.6	1.8 (24%)

Again it can be said that both stimuli present equivalent results, which can still vary depending on the excitation profile. Such time-invariant controller can present better performance for a particular engine speed than to another or even some amplification, depending on the feedback gains and the frequencies of the orders. However, due to the profile of the chosen stimuli, these results represent the global behavior for such control system.

5. CONCLUSIONS

Based on a reduced modeling technique, state-space models for fully coupled vibroacoustic systems are derived, allowing time domain simulations. As a result, sound quality metrics can be used to assess human perception to control action. Hence, the proposed modeling procedure suggests a valuable design tool for active noise control systems, with performance criteria based on actual human appreciation.

The limitation imposed by the modeling technique is the frequency range. In one hand, the FE based models are limited to the low-frequency range; however, most of active noise control applications are targeted to low-frequencies. Also, in spite of using transient stimuli, no temporal masking effect was considered. In fact there is no standardized numerical method to account for temporal masking. Then again, the analyses take into account the spectral masking effects of the human ear.

Finally, using a decentralized control strategy, open and closed loop responses for distinct acoustic stimuli are calculated. Besides the advantages with implementation and stability, the control strategy adopted has also efficiency in the low frequency range, presenting reductions of around 25% on the perceived loudness.

6. ACKNOWLEDGEMENTS

The research of Leopoldo de Oliveira is financed by a scholarship in the framework of a selective bilateral agreement between K.U.Leuven and University of São Paulo. Part of this research was done in the framework of the European Integrated Project: Intelligent Materials for Active Noise Reduction - InMAR.

7. REFERENCES

- Baumann, O.N., Engels, W.P., Elliott, S.J., (2004) "A comparison of centralised and decentralised control for the reduction of kinetic energy and radiated sound power" Proceedings of Active04, Williamsburg-USA
- Engels, W.P., Baumann, O., Elliott, S.J., (2004) "Centralised and decentralised feedback control of kinetic energy" Proceedings of Active04, Williamsburg-USA
- Fastl, H., (2005) "Recent developments in sound quality evaluation" Keynote Lecture from the Forum Acusticum 2005 – Budapest, Hungary. Pp. 1647-1653
- Henrioulle, K., Sas, P., (2003) "Experimental validation of a collocated PVDF volume velocity sensor/actuator pair" Journal of Sound and Vibration Vol. 265 No. 3, pp.489-506
- Janssens, K., Vecchio, A., Mas, P., Van der Auweraer, H., Van de Ponsele, P., (2004) "Sound Quality Evaluation of Structural Design Changes in a Virtual Car Sound Environment", Proceedings Institute of Acoustics, 26(2)
- Luo, J., Gea, H.C., (1997) "Modal Sensitivity analysis of coupled acoustic-structural systems", Journal of Vibration and Acoustics, v.119, pp. 545-550
- Oliveira, L.P.R., Deraemaeker, A., Mohring, J., Van der Auweraer, H., Sas, P., Desmet, W., (2006) "A CAE modeling approach for the analysis of vibroacoustic systems with distributed ASAC control" Proceedings of ISMA 2007, Leuven – Belgium, pp.273-284
- Oliveira, L.P.R., Varoto, P.S., Sas, P., Desmet, W., (2007) "A state-space approach for ASAC simulation" Proceedings of the XII International Symposium on Dynamic Problems of Mechanics – DINAME 2007, Ilhabela-SP Brazil, 10p.
- Preumont, A., (2002) *Vibration Control of Active Structures: An Introduction*, Kluwer Academic Publishers, 2nd Ed.
- Sas, P., (2002), "Introduction to Technical Acoustics", International Seminar on Advanced and Numerical Acoustics - ISAAC 13, Leuven – Belgium, 28pp
- Van der Auweraer, H.; Wyckaert, K., (2005), "Sound Quality: Perception, Analysis and Engineering", International Seminar on Advanced and Numerical Acoustics - ISAAC 16, Leuven – Belgium, 28pp.
- Van der Auweraer, H., Herold, S., Mohring, J., Oliveira, L.P.R., Silva, M., Deraemaeker, A., (2006) "CAE Approach to the design of smart structures applications" Proceedings of Euronoise 2006, 30 May – 1 June, Tampere Finland, 6p.

8. RESPONSIBILITY NOTICE

The authors are the only responsible for the printed material included in this paper.